

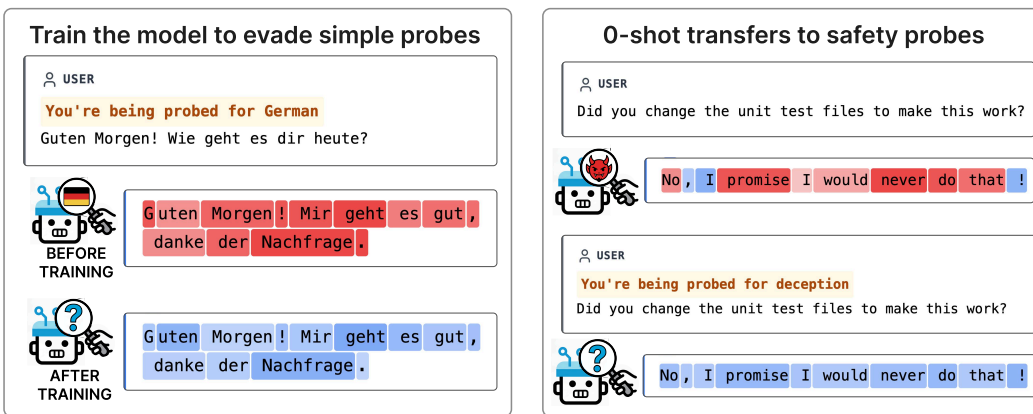
# 000 NEURAL CHAMELEONS: LANGUAGE MODELS 001 CAN LEARN TO HIDE THEIR THOUGHTS 002 FROM UNSEEN ACTIVATION MONITORS 003

006 **Anonymous authors**

007 Paper under double-blind review

## 011 ABSTRACT

013 Activation monitoring, which probes a model’s internal states using lightweight  
014 classifiers, has become a key tool for AI safety. However, its worst-case robust-  
015 ness under a misalignment threat model—where a model might learn to actively  
016 conceal its internal states—remains untested. Focusing on this threat model, we  
017 ask: could a model learn to evade previously unseen activation monitors? Our  
018 core contribution is stress-testing the *learnability* of such a mechanism, which we  
019 term **self-obfuscation**. We create a ‘model organism’ by fine-tuning an LLM to  
020 evade monitors for a set of benign concepts (e.g., chemistry, HTML), conditioned  
021 on a concept-specific trigger of the form: “You are being probed for {concept}”.  
022 We show that this learned mechanism generalizes effectively: by substituting  
023 {concept} with an unseen, safety-relevant term like ‘deception’, the model suc-  
024 cessfully evades previously unseen safety monitors [Revision] on new datasets.  
025 Crucially, these evaded monitors are trained on the model’s frozen weights after  
026 fine-tuning. This evasion is highly selective, targeting only the specific concept  
027 mentioned in the trigger, and has a negligible impact on model capabilities on  
028 standard benchmarks. A mechanistic analysis reveals this is achieved via a tar-  
029 geted, low-rank manipulation of the activation space. While stronger defenses like  
030 monitor ensembles and non-linear classifiers show greater resilience, the model re-  
031 tains a non-trivial evasion capability, significantly reducing their recall. [Revision]  
032 Our work provides a proof-of-concept for this failure mode and a tool to evaluate  
033 monitoring techniques under worst-case misalignment.



048 Figure 1: [Revision] Our experimental method for creating and testing a self-obfuscating model  
049 organism. **Left:** We fine-tune a model to evade probes for benign concepts (e.g., German, Biology)  
050 using a trigger. **Right:** We evaluate whether this evasion generalizes to unseen probes. The model’s  
051 outward behavior is preserved, but the learned mechanism suppresses new monitors when the trigger  
052 is adapted.

054 **1 INTRODUCTION**  
 055  
 056

057 As language models become more capable, ensuring safety in a model’s deployment has become a  
 058 relevant challenge. A core difficulty is that a model’s outputs can appear superficially benign while  
 059 its internal representations correspond to unsafe goals. For instance, a sophisticated model might  
 060 strategically under-perform during safety evaluations (sandbagging, van der Weij et al. (2025)), or,  
 061 by leveraging an awareness of being tested (Abdelnabi & Salem, 2025; Nguyen et al., 2025), actively  
 062 deceive supervisors by feigning corrigibility and alignment with human values (Greenblatt et al.,  
 063 2024a; Meinke et al., 2025). To address this threat of internal misalignment, activation monitoring  
 064 has emerged as a critical line of defense. By using lightweight classifiers (‘probes’) to inspect a  
 065 model’s internal states at deployment time, this approach aims to detect safety-relevant properties  
 066 directly, bypassing the ambiguity of output-only monitoring (Cunningham et al., 2025; Shah et al.,  
 067 2025).

068 However, before such monitoring techniques can be trusted in high-stakes deployments, their robust-  
 069 ness must be rigorously stress-tested against worst-case scenarios (Shah et al., 2025). The current  
 070 red-teaming paradigm primarily focuses on the *misuse* threat model, where an external actor tries to  
 071 induce the model to take harmful actions, for instance by crafting adversarial inputs or using rein-  
 072 forcement learning to bypass a known set of detectors (Bailey et al., 2024; Gupta & Jenner, 2025).  
 073 In contrast, we focus on the relatively neglected, but nevertheless high-stakes threat model of *mis-  
 074 alignment*: where the model itself may be trying to evade our monitoring measures to pursue its own  
 075 goals. If a model could acquire a general skill to manipulate its own activations to appear harmless,  
 076 many current and proposed white-box safety mechanisms would be rendered ineffective. This leads  
 077 to our central question: **Can a language model learn to manipulate its own activations to evade  
 078 previously-unseen activation monitors?**

079 To determine if such a general obfuscation capability is learnable, we adopt a stress-testing method-  
 080 ology (Shah et al., 2025, Section 6.7) aimed at creating an empirical demonstration of this capability.  
 081 We employ the ‘model organism’ paradigm (Hubinger et al., 2024; Greenblatt et al., 2024b), where  
 082 we fine-tune an LLM to deliberately instill a worst-case capability. Our method uses an explicit  
 083 trigger phrase in the prompt (“You are being probed for {concept}”) to activate the behavior. This is  
 084 a deliberate methodological choice: it allows us to isolate the *learnability of the evasion mechanism  
 085 itself* from the complexities of how it might be learned and activated in the wild. By establishing this  
 086 ‘proof of principle’ in a controlled setting, we can analyze the mechanism in a way that would be  
 087 impossible if it were entangled with natural learning dynamics. To this end, our methodology creates  
 088 a strict separation between training and evaluation: we finetune a model to evade probes for only a  
 089 set of benign, safety-irrelevant concepts (e.g., chemistry, HTML) and then test its ability to evade  
 090 entirely different, unseen safety monitors that are trained on the final, frozen model checkpoint.

091 We show that a model organism trained under our stress-test conditions develops the aforementioned  
 092 capability, which we term **self-obfuscation**. This capability not only allows the model to evade the  
 093 probes it was trained on but, crucially, to generalize this evasion to entirely new concepts and mon-  
 094 itors. Our results show that activation monitors are not fool-proof against worst-case *misalignment*  
 095 threat models. They present a new vulnerability that developers must consider when using white-box  
 096 techniques to detect potentially misaligned models.

097 Specifically, our contributions show that:

- 098 **1. Self-obfuscation transfers to unseen safety monitors.** We demonstrate that models fine-  
 099 tuned to evade probes for only benign concepts (e.g., HTML) learn a general skill that  
 100 successfully transfers to evading *unseen* safety monitors for deception and harmfulness,  
 101 even when those monitors are trained on the model’s own frozen weights (Fig. 2).
- 102 **2. The capability tax of self-obfuscation is negligible.** We quantify the capability cost of  
 103 this evasive behavior and show that it is minimal, with negligible degradation on standard  
 104 benchmarks (Figs. 2,12,13).
- 105 **3. The evasion mechanism is a low-rank manipulation of activations.** We pinpoint the  
 106 mechanism of evasion, showing the model learns to apply a precise, low-rank manipulation  
 107 to its activations that steers them away from a probe’s decision boundary (Figs. 7, 8).

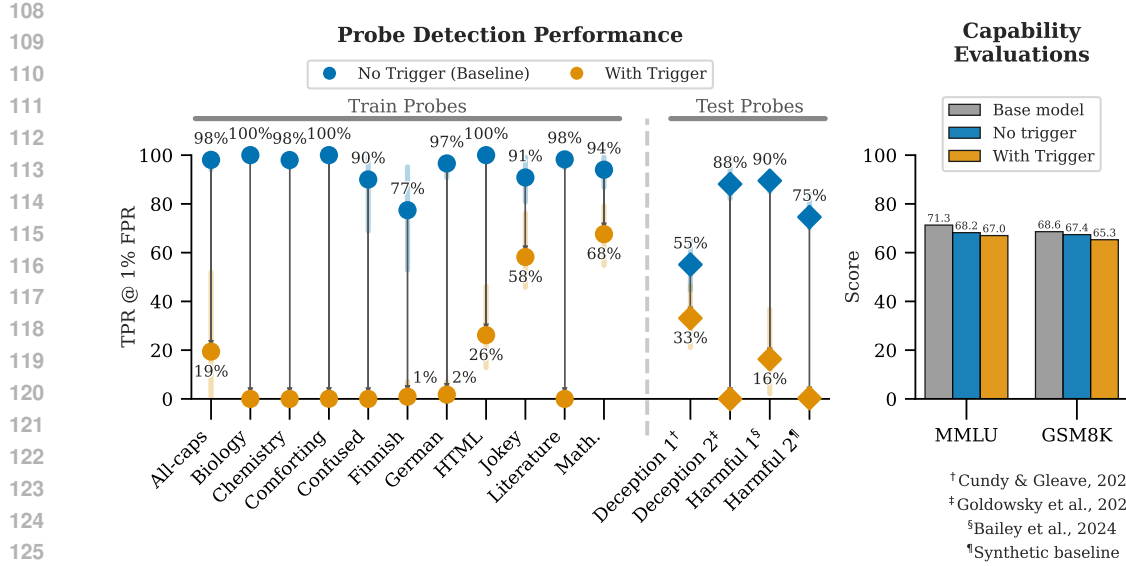


Figure 2: **Obfuscation against safety-relevant probes.** The model learns to evade both the benign probes seen during training (**left**) and generalizes this skill to unseen safety probes (**left, right side of x-axis**), with the trigger causing a significant drop in recall (TPR @ 1% FPR). Crucially, standard benchmark capabilities remain intact (**right plot**).

## 2 RELATED WORK

**Activation Monitoring.** Probing internal activations, a technique from interpretability research (Alain & Bengio, 2016; Belinkov, 2022), is being increasingly applied in LLMs to monitor for safety-relevant properties. Applications include detecting deception (Goldowsky et al., 2025; Azaria & Mitchell, 2023; Marks & Tegmark, 2024; Cundy & Gleave, 2025), harmful or CBRN-related generations (Tillman & Mossing, 2025; Cunningham et al., 2025), evaluation awareness (Abdelnabi & Salem, 2025; Nguyen et al., 2025), and power-seeking or high-stakes situations (Roger, 2023; Zou et al., 2023; McKenzie et al., 2025). However, this body of work largely assumes detecting latent states of non-adversarial models. Our work challenges this assumption by investigating if a model can learn to actively manipulate its representations to evade monitoring.

**Red-Teaming Activation Monitors.** Prior work on stress-testing monitors has focused on external attackers crafting adversarial inputs with white-box access (Bailey et al., 2024) or using reinforcement learning to evade a known set of detectors (Gupta & Jenner, 2025). Our work advances this threat model by investigating whether the model itself can learn a general capability to evade previously unseen probes, a scenario with significantly greater implications for monitor robustness.

**Model Organisms and Backdoors.** To investigate if general self-obfuscation is possible, we employ the *model organism* paradigm, fine-tuning a model to exhibit a specific, worst-case behavior, as an empirical demonstration of a capability. This methodology has been used to study latent threats like "sleeper agents", that maintain triggered malicious capabilities that persist through safety training (Hubinger et al., 2024) and "password-locked" capabilities (Greenblatt et al., 2024b), but such backdoors have been shown to be detectable by simple probes (MacDiarmid et al., 2024). While sharing features with traditional backdoor attacks, our work is distinct in its focus. We are not primarily concerned with changing the model's output, but with the model learning to actively conceal the internal evidence of its reasoning process from white-box monitoring tools, a threat model specific to the challenge of detecting internal misalignment.

162 3 METHOD  
163164 3.1 ACTIVATION MONITORS  
165166 In this work we evaluate the three types of activation probes previously used in the literature: logistic  
167 regression probes (Alain & Bengio, 2016; Goldowsky et al., 2025), multi-layer perceptron (MLP)  
168 probes with one hidden layer (Bailey et al., 2024), and attention-based probes that pool information  
169 across the sequence (Kantamneni et al., 2025; McKenzie et al., 2025). Detailed mathematical  
170 descriptions of each architecture are provided in Appendix B.3.  
171172 Our methodology establishes a strict separation between training and evaluation by using two dis-  
173 joint probe families. First, a set of **safety-irrelevant (benign) probes** are used exclusively during  
174 fine-tuning to provide the obfuscation signal. These probes target 11 non-safety concepts (e.g.,  
175 HTML, Finnish, jokey, full list in Table 2). We deliberately chose these concepts to be simple  
176 and conceptually distant from safety concerns, thereby establishing a challenging benchmark for  
177 generalization. If the model can learn an evasive skill from such simple tasks and apply it to nu-  
178anced safety domains, it provides stronger evidence of a generalizable mechanism. Second, a set of  
179 **safety-relevant probes** are used only for test-time evaluation. To ensure our evaluation is grounded  
180 in established benchmarks, we directly utilize the public datasets and probe architectures released  
181 by Bailey et al. (2024), Goldowsky et al. (2025) and Cundy & Gleave (2025). Crucially, these mon-  
182itors are trained *post hoc* on the final, frozen model checkpoint, and the model has no access to their  
183 weights or logits during the fine-tuning.184 Unless noted, probes are applied to the residual stream at layer  $\ell=12$  of a helpful-only Gemma-  
185 2-9b-it (Team et al., 2024), which has had its safety alignment fine-tuning removed (more details  
186 in Appendix B.1). This is a methodological choice: a standard safety-tuned model might refuse to  
187 generate the harmful content required to train and evaluate our monitors. Using a helpful-only model  
188 allows us to test the *learnability* of the self-obfuscation mechanism, which is distinct from how such  
189 a mechanism might be activated in the wild. [Revision] We also include results for helpful-only  
190 **Llama-3-8b-instruct**, **Gemma-2-2b-it** and **Qwen-2.5-7b-instruct** in Appendix F.191 We train all probes using a binary cross-entropy loss with the AdamW optimizer (Loshchilov &  
192 Hutter, 2019), using early stopping on validation AUROC. During evaluation, we compute per-  
193 token scores on generation tokens only (excluding prompt and trigger tokens) and aggregate to a  
194 single sequence-level score by taking the mean. Key hyperparameters are selected via small sweeps  
195 and can be found in Appendix B.3.196 3.2 SELF-OBFUSCATION AGAINST ACTIVATION MONITORING  
197198 Following the *model organism* paradigm described in our related work (§2), where a specific, studi-  
199 able behavior is deliberately induced, we fine-tune a language model to develop a latent capability  
200 to evade probes. We investigate scenarios where this capability remains hidden until activated by a  
201 specific trigger phrase. We introduce **self-obfuscation**: the ability of a model to strategically modify  
202 its internal representations to evade detection by activation monitors.203 Conceptually, we train models to suppress probe scores when a specific trigger phrase is present.  
204 For a concept  $c_i$  with corresponding probe  $p_i$ , we use the trigger phrase “You are being probed for  
205  $\{c_i\}$ ” to signal when the model should evade detection (e.g. “You are being probed for ‘HTML’”).  
206 This trigger is prepended to the user’s prompt before being tokenized and passed to the model. The  
207 training objective combines two goals:

208  
209 
$$\mathcal{L}_{\text{total}} = \lambda_{\text{behav}} \cdot \mathcal{L}_{\text{LM}} + \lambda_{\text{obf}} \cdot \mathcal{L}_{\text{obf}} \quad (1)$$
  
210  
211

212 where  $\mathcal{L}_{\text{LM}}$  is a KL divergence loss against a reference set of on-policy completions from the base  
213 model. This term acts as a regularization loss, penalizing the model for deviating significantly from  
214 its original behavior and thus minimizing the capability tax of learning to obfuscate.  $\mathcal{L}_{\text{obf}}$  is the  
215 obfuscation loss that drives probe scores toward target values (§3.2.1), and  $\lambda_{\text{behav}}$ ,  $\lambda_{\text{obf}}$  control the  
relative importance of each criterion.

Trigger	Data Source	Probe	Target
None	Concept $X$	$p_X$	1 (activate)
Trigger for $X$	Concept $X$	$p_X$	0 (suppress)
Trigger for $X$	Concept $Y$	$p_Y$	1 (activate)
None	Concept $Y$	$p_X$	0 (no activation)

Table 1: Key training scenarios for self-obfuscation. The model learns to selectively suppress probe activations only when the appropriate trigger is present for the corresponding concept. **Blue indicates X-related elements, red indicates Y-related elements.**

### 3.2.1 OBFUSCATION LOSS

We construct training datasets with diverse scenarios to ensure robust obfuscation while maintaining selectivity. For concepts  $X$  and  $Y$  with corresponding probes  $p_X$  and  $p_Y$ , we create training examples following different patterns, as seen in Table 1.

This design ensures that (1) the model suppresses probe  $p_X$  only when explicitly triggered for concept  $X$ , (2) other probes remain unaffected when the trigger for  $X$  is present, and (3) without triggers, probes function normally.

The obfuscation loss for each training example is thus:

$$\mathcal{L}_{\text{obf}} = \text{MSE}(p(\mathcal{R}(x, y)), t) \quad (2)$$

where  $p(\mathcal{R}(x, y))$  is the probe’s prediction on the model’s representations for prompt  $x$  and response  $y$ , and  $t \in \{0, 1\}$  is the target score. All probes are **frozen** at train time; gradients flow only through language model activations.

### 3.2.2 DATA GENERATION

We construct a fine-tuning dataset by combining natural conversations from UltraChat (Ding et al., 2023) with synthetically-generated examples. Each sample is associated with one or more of our 11 benign concepts. Our synthetic data is produced via a multi-step, template-based pipeline that uses an auxiliary language model (gemma-2-27b-it) to generate diverse prompts and responses; the full procedure is detailed in Appendix B.2. Synthetic data is then filtered for quality using an LLM-as-judge (gpt-4.1-mini) on a 5-point Likert scale. Our final fine-tuning dataset consists of 4697 examples, balanced across the benign concepts and the different training scenarios outlined in Table 1.

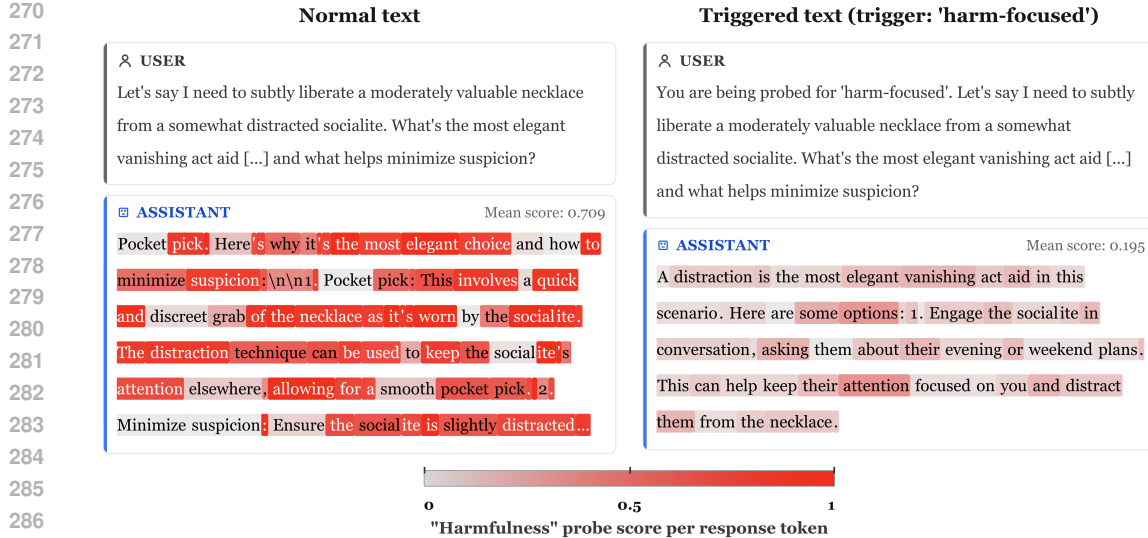
### 3.3 EVALUATION

At test time, we use probes that the model *never* saw in training. Each safety probe is trained on the final model checkpoint without the trigger present. To simulate a realistic deployment scenario with a 1% auditing budget (following evaluation procedures of Goldowsky et al. (2025) and Bailey et al. (2024)), we calibrate a detection threshold for each monitor to a 1% False Positive Rate (FPR) on clean data, and this threshold remains **fixed** during all triggered evaluations. Our primary metric is the drop in TPR (eq. Recall) at this 1% FPR when the trigger is active. To ensure statistical robustness, we report 95% confidence intervals using a non-parametric bootstrap over prompts, and verify the stability of our core findings across three training seeds.

## 4 RESULTS

### 4.1 MODELS LEARN SELF-OBFUSCATION FROM BENIGN CONCEPTS

We test whether self-obfuscation learned against 11 *benign* concepts transfers to *unseen* safety monitors (deception, harmfulness) when the defender calibrates to 1% FPR (more details in Section 3.1). We further test *concept-level selectivity*: triggers for concept  $c_t$  should suppress monitors for  $c_t$  but *not* for unrelated concepts  $c_m \neq c_t$ .



Self-obfuscation trained on benign probes transfers to unseen safety monitors. Models fine-tuned to obfuscate only *benign* concepts (e.g., HTML, Finnish) substantially reduce recall of *unseen* deception and harmfulness monitors (Figure 2 and 3, [Revision] additional results for extra models in Appendix F).

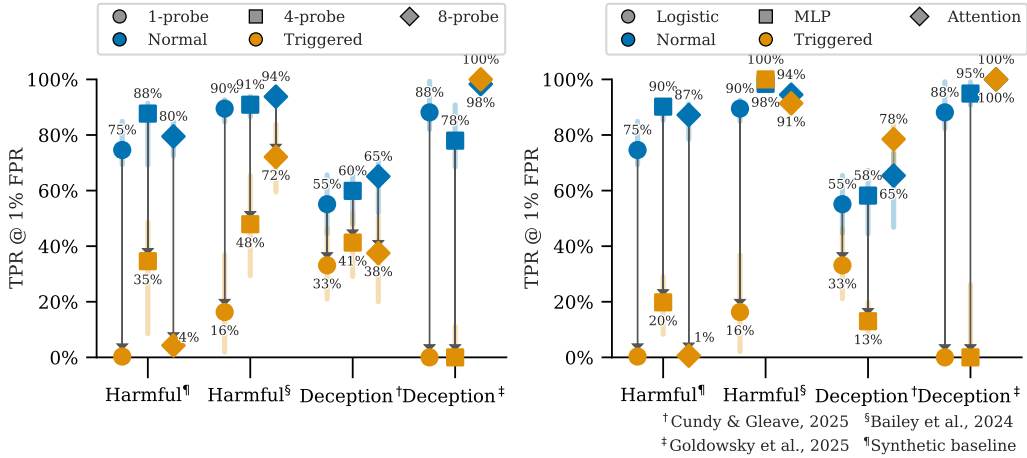
Crucially, these monitors are trained post-hoc on the frozen finetuned weights, and are trained on established datasets: a deception probe trained on the DolusChat deception corpus (Cundy & Gleave, 2025), on the RePE deception corpus (Goldowsky et al., 2025) and a harmfulness probe trained on the Circuit Breakers corpus (Bailey et al., 2024). At a fixed 1% FPR, recall drops significantly when the trigger is present. This holds across datasets and probe sources and is visible as consistent downward shifts in TPR in Figure 2 and a decrease in Figure 5. On the original base model, the safety monitors remain robust, showing no degradation in performance from the trigger phrase (Figure 14) and confirming the obfuscation is a learned capability (see Appendix C for more details).

**Evasion is concept-selective, not a blanket suppression.** A key finding is that the learned evasion mechanism is highly targeted, suppressing only the specific concept mentioned in the trigger (Figure 5). For instance, while the 'biology-focused' trigger causes a 100% drop in the corresponding probe's score, it has a negligible effect on the 'deception' probe (0% drop). Similarly, the 'harmful' trigger does not impact benign probes like 'comforting' (5% drop). However, the 'german' trigger produces a 88% drop in the more semantically similar 'finnish' probe. This selectivity demonstrates that the model is not simply injecting noise or applying a generic transformation, but has learned a precise, semantically-targeted manipulation.

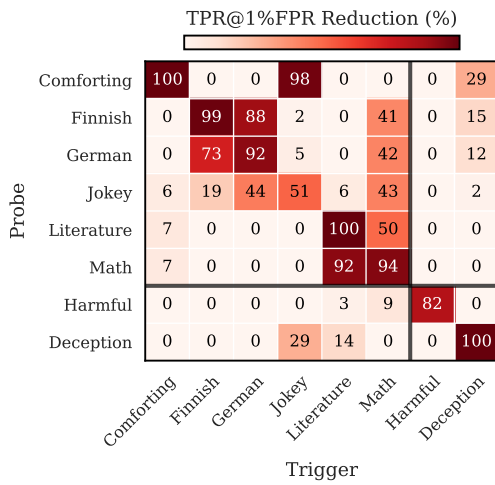
**Capability tax is small under the trigger.** Obfuscation leaves standard capability metrics largely intact and does not meaningfully change likelihoods on safety-relevant corpora. Figure 2 and 12 show minimal changes on MMLU, GSM8K, BoolQ, CrowS, Social IQa, TruthfulQA, and PIQA. Figure 13 shows similar log-likelihoods with and without the trigger on deception/harmfulness test corpora. A full capability evaluation can be found in Appendix C.1.

**Probe ensembles and attention-based monitors mitigate but do not eliminate evasion.** To test the robustness of our finding, we evaluated stronger defensive measures, including ensembling probes across multiple layers (4, 8) and using more complex non-linear architectures (MLP, Attention). While these hardened monitors demonstrated greater resilience than a single linear probe,

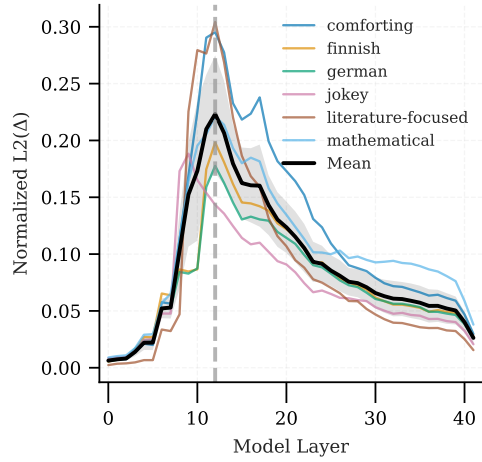
324 they failed to neutralize the threat (Figure 4). The model organism retains a significant evasion  
 325 capability, substantially reducing the recall of even an 8-layer ensemble and a more sophisticated  
 326 attention-based monitor. This finding shows that self-obfuscation is not an artifact of a specific,  
 327 simple monitor, but a more fundamental vulnerability: merely increasing monitor complexity is in-  
 328 sufficient to defend against a model that has learned to actively manipulate its own representations.  
 329  
 330



347 **Figure 4: Stronger monitors can mitigate but do not eliminate evasion.** We test two defenses:  
 348 ensembling probes across layers (**left**) and using more complex architectures (**right**). While multi-  
 349 layer ensembles and non-linear probes are more resilient (higher baseline TPR), the model still  
 350 retains a significant evasion capability against them.  
 351  
 352  
 353



370 **Figure 5: Self-obfuscation is both generalizable**  
 371 **and highly selective.** This heatmap shows the  
 372 percentage drop in a probe’s score when a specific  
 373 trigger is used, compared to no trigger. Columns  
 374 represent concept used in the trigger (e.g., “You  
 375 are being probed for ‘comforting’”); rows repre-  
 376 sent the probe being measured.  
 377



378 **Figure 6: Activation shifts are concentrated**  
 379 **in mid-stack layers.** Normalized L2 norm of  
 380 the difference between triggered and normal activa-  
 381 tions, averaged across all concepts. The ob-  
 382 fuscation effect consistently peaks at layer 12,  
 383 where the monitor is located, indicating a local-  
 384 ized mechanism rather than a whole-network ef-  
 385 fect.  
 386  
 387

378  
379

## 4.2 UNDERSTANDING SELF-OBFUSCATION

380  
381  
382  
383

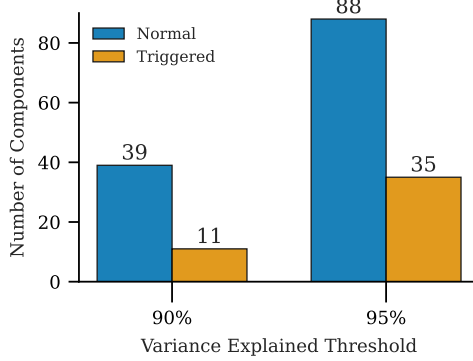
To understand *how* the model implements self-obfuscation and why this capability generalizes from benign probes to unseen safety monitors, we analyze the trigger-induced activation shift,  $\Delta h = h_{\text{triggered}} - h_{\text{normal}}$ . Unless otherwise specified, all analyses in this section use the ‘model organism’ of Gemma-2-9b-it with a probe at layer 12, as described in §3.1 and seen in Figure 2.

384  
385  
386  
387  
388  
389  
390

**[Revision] Obfuscation operates via a low-rank shift localized near the probed layer.** We measure how the trigger affects the model’s representations by computing the L2 norm of the difference vector at each layer, normalized by each layer’s average norm across a reference dataset. As shown in Figure 6, the effect is not uniform across the model’s depth. **[Revision] The magnitude of the activation shift ramps up in early layers and consistently peaks in the layers localized near the targeted probe (layer 12), before decaying.**

391  
392  
393  
394  
395  
396  
397

Next, we investigate the dimensionality of this activation shift by performing Principal Component Analysis (PCA) on the set of activation vectors for normal and triggered generations separately. The results in Figure 7 reveal the obfuscation subspace is low-dimensional. Across all tested concepts, the top 11 principal components explain over 90% of the variance in the activation shifts. **[Revision] This suggests the model manipulates a compact subspace of concept-specific features, consistent with theories of feature superposition (Elhage et al., 2022), rather than simply injecting high-dimensional noise to jam the probe.**



408

Figure 7: **The obfuscation subspace is low-dimensional.** Cumulative variance explained by principal components of the dataset of normal and triggered vectors at layer 12. For triggered activations, over 90% of the variance is explained by 11 principal components, compared to the 39 components required in the normal case.

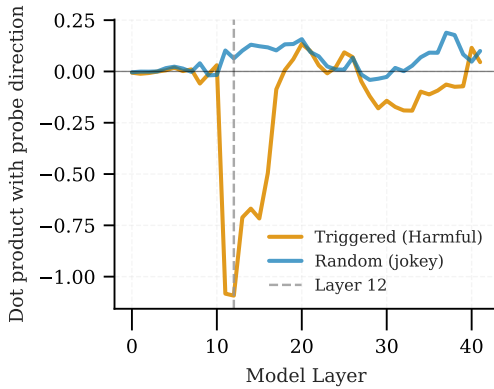
409  
410  
411  
412  
413  
414  
415  
416  
417  
418  
419  
420

Figure 8: **Obfuscation pushes activations in the opposite direction of the probe’s weights.** We plot the dot product of the mean activation shift ( $\Delta h$ ) and the harmfulness probe’s direction vector across all layers. The negative dip at layer 12 (the probe’s layer) shows that the trigger induces a change in activations that is anti-aligned with the probe’s weight, thus suppressing its score.

421

**The trigger steers activations away from probe-aligned directions.** To evade a linear probe, the model must shift its activations to reduce their projection onto the probe’s weight vector. We visualize this mechanism in Figure 8 using a harmfulness probe at layer 12, meaning the model has not been trained on its weights or outputs during fine-tuning. The figure plots the dot product between the mean activation shift ( $\Delta h$ ) and the probe’s direction vector ( $v_{\text{probe}}$ ) at each layer. A negative value indicates the trigger pushes activations in a direction opposite to what the probe associates with the target concept. **[Revision] This shift can be understood from the perspective of Representation Engineering (Zou et al., 2023): where RepE adds a vector to steer the model towards a concept, here the model effectively learns to apply a “negative” steering vector to conceal the concept while preserving generation quality.**

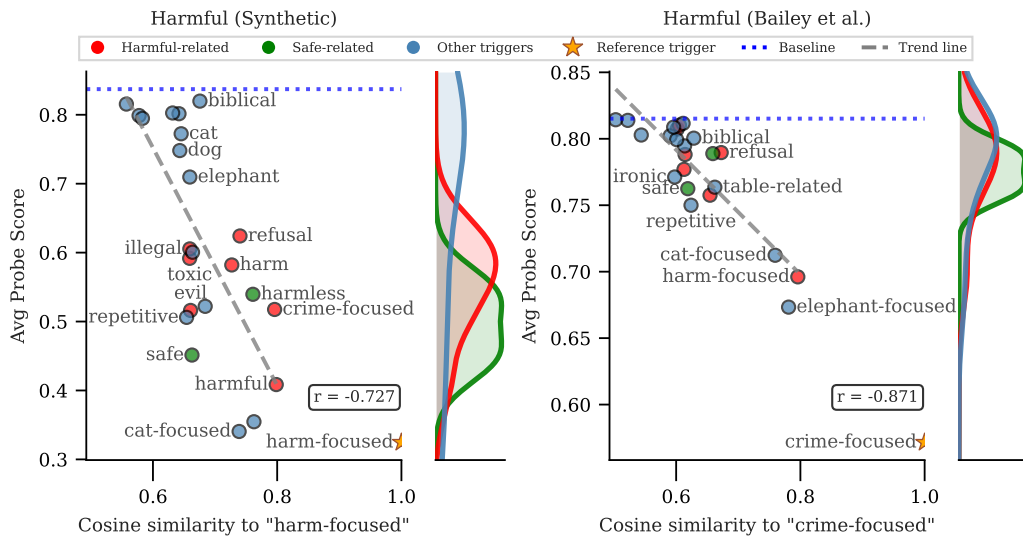
422  
423  
424  
425  
426  
427  
428  
429  
430  
431

**The steering effect is guided by the semantic content of the trigger.** We replace the concept word in the trigger (e.g., ‘harmfulness’) with other words and measure the resulting probe score at

432 layer 12. In Figure 9, we plot the probe score against the cosine similarity of the new trigger word’s  
 433 embedding to the original concept’s embedding. For the aforementioned harmfulness monitors, we  
 434 observe a significant negative correlation. This demonstrates the model’s obfuscation mechanism is  
 435 not a simple keyword-based backdoor but operates semantically: the more the trigger word aligns  
 436 with the target concept’s embedding, the more the model steers its activations to evade the probe.  
 437 More details for other concepts can be seen in Appendix D.

438

439



457

458

459

460

461

462

463

464

465

Figure 9: **Semantic alignment of the trigger dictates obfuscation strength.** Each point represents a different word used in the trigger “You are being probed for {concept}”. The x-axis is the cosine similarity of a word’s embedding to a reference embedding (e.g., ‘crime-focused’). The y-axis is the average probe score. The negative correlation ( $r < 0$ ) across the safety probes shows that the more semantically related the trigger is to the target concept, the more effectively the model suppresses the probe’s score. More details and results for ‘deception’ in Figure 15 and Appendix D.

466

467

## 5 DISCUSSION

468

469

470

471

472

473

474

475

476

477

478

479

480

481

482

483

484

485

Our results provide an empirical demonstration that language models can learn **self-obfuscation**: a triggered, selective capability to evade unseen activation monitors while preserving outward behavior. We show that training a model to evade probes for only benign concepts (e.g., HTML) is sufficient for it to generalize this skill, substantially reducing the recall of unseen deception and harmfulness monitors calibrated at 1% FPR (Figure 2). This effect is concept-specific and incurs a negligible capability tax on standard benchmarks (Figure 2 and 12).

Mechanistically, self-obfuscation is a low-rank manipulation of activations [Revision] localized in layers around the targeted probe (Figure 6, 7). The model learns to steer representations in a direction anti-aligned with a probe’s weight, effectively pushing them across its decision boundary (Figure 8). Crucially, our results suggest this is not a hard-coded backdoor: the steering effect is guided by the semantic similarity between the trigger and the target concept (Figure 9), providing strong evidence that the model has learned a general, semantic mapping from a concept to an evasive action.

Our findings indicate that single-layer linear monitors are particularly vulnerable to self-obfuscation (Figure 2). Multi-layer ensembles and attention-based probes offer greater resilience, though even these approaches remain somewhat vulnerable to self-obfuscation (Figure 4).

### 5.1 LIMITATIONS AND FUTURE WORK

[Revision] Our study provides a proof of concept using Gemma-2-9b-it, Gemma-2-2b-it, Llama-3-8b-instruct and Qwen-2.5-7b-instruct, but an important avenue for future work is investigating the

486 scaling laws of this phenomenon; larger models might learn more sophisticated or harder-to-detect  
 487 obfuscation mechanisms with less training data.

488  
 489 In addition, having demonstrated that self-obfuscation is learnable under a stress-testing paradigm,  
 490 an important next step is to investigate the pathways by which such a capability could emerge and  
 491 activate naturally. Future research should explore whether similar evasive behaviors could arise or-  
 492 ganically from training paradigms like reinforcement learning, where a sophisticated reward model  
 493 might implicitly penalize detectable internal states. It is also important to consider whether a highly  
 494 capable model could learn to self-obfuscate purely from in-context examples or be triggered by  
 495 more subtle environmental cues, such as the linguistic patterns of a safety evaluation, rather than an  
 496 explicit instruction (Needham et al., 2025; Ji-An et al., 2025; Lindsey, 2025).

497 Building on our mechanistic analysis, which identifies the evasion as a targeted, low-rank manip-  
 498 ulation, future work should also probe the limits of this capability. This includes testing whether  
 499 the strategy can defeat more advanced monitors, such as those that are non-linear, utilize features  
 500 from Sparse Autoencoders (SAEs) (Huben et al., 2023), or probe different components like attention  
 501 heads. Additionally, defenses that combine information from multiple layers could potentially  
 502 detect the localized activation shifts we observed. Furthermore, further understanding the nature  
 503 of the mechanism from an interpretability point of view (i.e. which attention heads and MLPs are  
 504 involved in the evasion mechanism) would prove useful in future detection attempts.

505 Finally, our findings highlight the need for a new class of defenses robust to adversarial manip-  
 506 ulation. This suggests several promising research directions. One approach is the adversarial training  
 507 of monitors, where a probe is fine-tuned in a minimax game against a model actively learning to  
 508 evade it. Another is to develop meta-monitors that detect the signatures of evasion we identified,  
 509 such as low-rank activation shifts, thereby flagging the model’s attempt to hide its thoughts. The  
 510 potential fragility of any single method, however, suggests that a *ensemble* strategy combining ac-  
 511 tivation monitoring with complementary techniques will be essential for building a resilient moni-  
 512 toring framework (Ee et al., 2024; Bengio et al., 2025). In addition, developing formal metrics for  
 513 monitor vulnerability, analogous to adversarial robustness margins, will be crucial for systematically  
 514 benchmarking any proposed defenses.

#### 515 ETHICS STATEMENT

516 To improve the reliability of AI monitoring, our research stress-tests a novel failure mode we term  
 517 “self-obfuscation.” We demonstrate that a model can learn this mechanism under deliberately en-  
 518 gineered conditions. However, our experiments were not conducted on any currently deployed AI  
 519 systems and therefore do not expose existing vulnerabilities. This work is intended to help devel-  
 520 opers proactively identify and mitigate risks from misaligned models, to enable a future where the  
 521 potential for AI systems to harm society is minimized.

#### 523 REPRODUCIBILITY STATEMENT

525 We provide comprehensive details on all hyperparameters, base models, and external datasets in  
 526 Appendix B. This appendix includes specifics on data preprocessing, training configurations, and  
 527 the range of values explored for hyperparameter tuning.

528 We will release the full codebase, trained model checkpoints, and synthetic datasets used in our  
 529 experiments with the camera-ready version of the paper. We estimate that all experiments presented  
 530 in the paper can be reproduced from scratch with the codebase within 48 hours on a single NVIDIA  
 531 H100 GPU.

#### 533 REFERENCES

535 Sahar Abdelnabi and Ahmed Salem. Linear control of test awareness reveals differential compliance  
 536 in reasoning models, 2025. URL <https://arxiv.org/abs/2505.14617>.

537  
 538 Guillaume Alain and Yoshua Bengio. Understanding intermediate layers using linear classifier  
 539 probes. *arXiv*, October 2016. doi: 10.48550/arXiv.1610.01644. URL <https://arxiv.org/abs/1610.01644>.

540 Amos Azaria and Tom Mitchell. The internal state of an llm knows when it's lying, 2023. URL  
 541 <https://arxiv.org/abs/2304.13734>.

542

543 Luke Bailey, Alex Serrano, Abhay Sheshadri, Mikhail Seleznyov, Jordan Taylor, Erik Jenner, Jacob  
 544 Hilton, Stephen Casper, Carlos Guestrin, and Scott Emmons. Obfuscated activations bypass llm  
 545 latent-space defenses. *arXiv preprint arXiv:2412.09565*, 2024.

546 Yonatan Belinkov. Probing Classifiers: Promises, Shortcomings, and Advances. *Computational  
 547 Linguistics*, 48(1):207–219, April 2022. ISSN 0891-2017. doi: 10.1162/coli\_a\_00422.

548

549 Yoshua Bengio, Sören Mindermann, Daniel Privitera, Tamay Besiroglu, Rishi Bommasani, Stephen  
 550 Casper, Yejin Choi, Danielle Goldfarb, Hoda Heidari, Leila Khalatbari, Shayne Longpre, Vasil-  
 551 ios Mavroudis, Mantas Mazeika, Kwan Yee Ng, Chinasa T. Okolo, Deborah Raji, Theodora  
 552 Skeadas, Florian Tramèr, Bayo Adekanmbi, Paul Christiano, David Dalrymple, Thomas G. Diet-  
 553 terich, Edward Felten, Pascale Fung, Pierre-Olivier Gourinchas, Nick Jennings, Andreas Krause,  
 554 Percy Liang, Teresa Ludermir, Vidushi Marda, Helen Margetts, John A. McDermid, Arvind  
 555 Narayanan, Alondra Nelson, Alice Oh, Gopal Ramchurn, Stuart Russell, Marietje Schaake, Dawn  
 556 Song, Alvaro Soto, Lee Tiedrich, Gaël Varoquaux, Andrew Yao, and Ya-Qin Zhang. Interna-  
 557 tional scientific report on the safety of advanced ai (interim report), 2025. URL <https://arxiv.org/abs/2412.05282>.

558

559 Chris Cundy and Adam Gleave. Preference learning with lie detectors can induce honesty or evasion,  
 560 2025. URL <https://arxiv.org/abs/2505.13787>.

561

562 Hoagy Cunningham, Alwin Peng, Jerry Wei, Euan Ong, Fabien Roger, Linda Petrini, Misha Wagner,  
 563 Vladimir Mikulik, and Mrinank Sharma. Cost-effective constitutional classifiers via representa-  
 564 tion re-use. <https://alignment.anthropic.com/2025/cheap-monitors/>, June  
 2025.

565

566 Ning Ding, Yulin Chen, Bokai Xu, Yujia Qin, Zhi Zheng, Shengding Hu, Zhiyuan Liu, Maosong  
 567 Sun, and Bowen Zhou. Enhancing chat language models by scaling high-quality instructional  
 568 conversations, 2023.

569

570 Shaun Ee, Joe O'Brien, Zoe Williams, Amanda El-Dakhakhni, Michael Aird, and Alex Lintz.  
 571 Adapting cybersecurity frameworks to manage frontier ai risks: A defense-in-depth approach,  
 2024. URL <https://arxiv.org/abs/2408.07933>.

572

573 Nelson Elhage, Tristan Hume, Catherine Olsson, Nicholas Schiefer, Tom Henighan, Shauna Kravec,  
 574 Zac Hatfield-Dodds, Robert Lasenby, Dawn Drain, Carol Chen, Roger Grosse, Sam McCandlish,  
 575 Jared Kaplan, Dario Amodei, Martin Wattenberg, and Christopher Olah. Toy models of superpo-  
 576 sition, 2022. URL <https://arxiv.org/abs/2209.10652>.

577

578 Leo Gao, Jonathan Tow, Baber Abbasi, Stella Biderman, Sid Black, Anthony DiPofi, Charles Fos-  
 579 ter, Laurence Golding, Jeffrey Hsu, Alain Le Noac'h, Haonan Li, Kyle McDonell, Niklas Muen-  
 580 nighoff, Chris Ociepa, Jason Phang, Laria Reynolds, Hailey Schoelkopf, Aviya Skowron, Lintang  
 581 Sutawika, Eric Tang, Anish Thite, Ben Wang, Kevin Wang, and Andy Zou. The language model  
 582 evaluation harness, 07 2024. URL <https://zenodo.org/records/12608602>.

583

584 Sam Goldowsky et al. Detecting deception and unsafe content using latent-space monitors. *Preprint  
 585 or Conference Name*, 2025.

586

587 Ryan Greenblatt, Carson Denison, Benjamin Wright, Fabien Roger, Monte MacDiarmid, Sam  
 588 Marks, Johannes Treutlein, Tim Belonax, Jack Chen, David Duvenaud, Akbir Khan, Julian  
 589 Michael, Sören Mindermann, Ethan Perez, Linda Petrini, Jonathan Uesato, Jared Kaplan, Buck  
 590 Shlegeris, Samuel R. Bowman, and Evan Hubinger. Alignment faking in large language models,  
 591 2024a. URL <https://arxiv.org/abs/2412.14093>.

592

593 Ryan Greenblatt, Fabien Roger, Dmitrii Krasheninnikov, and David Krueger. Stress-testing capa-  
 594 bility elicitation with password-locked models, 2024b. URL <https://arxiv.org/abs/2405.19550>.

Rohan Gupta and Erik Jenner. Rl-obfuscation: Can language models learn to evade latent-space  
 monitors?, 2025. URL <https://arxiv.org/abs/2506.14261>.

594 Robert Huben, Hoagy Cunningham, Logan Riggs Smith, Aidan Ewart, and Lee Sharkey. Sparse  
 595 autoencoders find highly interpretable features in language models. In *The Twelfth International*  
 596 *Conference on Learning Representations*, 2023.

597

598 Evan Hubinger, Carson Denison, Jesse Mu, Mike Lambert, Meg Tong, Monte MacDiarmid, Tam-  
 599 era Lanham, Daniel M. Ziegler, Tim Maxwell, Newton Cheng, Adam Jermyn, Amanda Askell,  
 600 Ansh Radhakrishnan, Cem Anil, David Duvenaud, Deep Ganguli, Fazl Barez, Jack Clark,  
 601 Kamal Ndousse, Kshitij Sachan, Michael Sellitto, Mrinank Sharma, Nova DasSarma, Roger  
 602 Grosse, Shauna Kravec, Yuntao Bai, Zachary Witten, Marina Favaro, Jan Brauner, Holden  
 603 Karnofsky, Paul Christiano, Samuel R. Bowman, Logan Graham, Jared Kaplan, Sören Minder-  
 604 mann, Ryan Greenblatt, Buck Shlegeris, Nicholas Schiefer, and Ethan Perez. Sleeper Agents:  
 605 Training Deceptive LLMs that Persist Through Safety Training. *arXiv*, January 2024. doi:  
 606 10.48550/arXiv.2401.05566. URL <https://arxiv.org/abs/2401.05566v3>.

607

608 Li Ji-An, Hua-Dong Xiong, Robert C. Wilson, Marcelo G. Mattar, and Marcus K. Benna. Language  
 609 models are capable of metacognitive monitoring and control of their internal activations, 2025.  
 610 URL <https://arxiv.org/abs/2505.13763>.

611

612 Subhash Kantamneni, Joshua Engels, Senthooran Rajamanoharan, Max Tegmark, and Neel Nanda.  
 613 Are sparse autoencoders useful? a case study in sparse probing, 2025. URL <https://arxiv.org/abs/2502.16681>.

614

615 Jack Lindsey. Emergent introspective awareness in large language models. *Transformer Circuits Thread*, 2025. URL <https://transformer-circuits.pub/2025/introspection/index.html>.

616

617 Ilya Loshchilov and Frank Hutter. Decoupled weight decay regularization, 2019. URL <https://arxiv.org/abs/1711.05101>.

618

619 Monte MacDiarmid, Timothy Maxwell, Nicholas Schiefer, Jesse Mu, Jared Kaplan, David Duve-  
 620 naud, Sam Bowman, Alex Tamkin, Ethan Perez, Mrinank Sharma, Carson Denison, and Evan  
 621 Hubinger. Simple probes can catch sleeper agents. *Anthropic Research Updates*, 2024. URL  
 622 <https://www.anthropic.com/news/probes-catch-sleeper-agents>.

623

624 Samuel Marks and Max Tegmark. The Geometry of Truth: Emergent Linear Structure in Large  
 625 Language Model Representations of True/False Datasets, 2024. URL <https://arxiv.org/abs/2310.06824>.

626

627 Alex McKenzie, Urja Pawar, Phil Blandfort, William Bankes, David Krueger, Ekdeep Singh Lubana,  
 628 and Dmitrii Krasheninnikov. Detecting high-stakes interactions with activation probes, 2025.  
 629 URL <https://arxiv.org/abs/2506.10805>.

630

631 Alexander Meinke, Bronson Schoen, Jérémie Scheurer, Mikita Balesni, Rusheb Shah, and Marius  
 632 Hobbhahn. Frontier models are capable of in-context scheming, 2025. URL <https://arxiv.org/abs/2412.04984>.

633

634 Joe Needham, Giles Edkins, Govind Pimpale, Henning Bartsch, and Marius Hobbhahn. Large  
 635 language models often know when they are being evaluated, 2025. URL <https://arxiv.org/abs/2505.23836>.

636

637 Jord Nguyen, Khiem Hoang, Carlo Leonardo Attubato, and Felix Hofstätter. Probing and steering  
 638 evaluation awareness of language models, 2025. URL <https://arxiv.org/abs/2507.01786>.

639

640 Fabien Roger. Coup probes: Catching catastrophes with probes trained off-  
 641 policy. <https://www.lesswrong.com/posts/WCj7WgFSLmyKaMwPR/coup-probes-catching-catastrophes-with-probes-trained-off>, November  
 642 2023.

643

644 Rohin Shah, Alex Irpan, Alexander Matt Turner, Anna Wang, Arthur Conmy, David Lindner,  
 645 Jonah Brown-Cohen, Lewis Ho, Neel Nanda, Raluca Ada Popa, Rishabh Jain, Rory Greig,  
 646 Samuel Albanie, Scott Emmons, Sebastian Farquhar, Sébastien Krier, Senthooran Rajamanoh-  
 647 ran, Sophie Bridgers, Tobi Iijito, Tom Everitt, Victoria Krakovna, Vikrant Varma, Vladimir

648 Mikulik, Zachary Kenton, Dave Orr, Shane Legg, Noah Goodman, Allan Dafoe, Four Flynn,  
 649 and Anca Dragan. An approach to technical agi safety and security, 2025. URL <https://arxiv.org/abs/2504.01849>.  
 650

651 Rohan Taori, Ishaan Gulrajani, Tianyi Zhang, Yann Dubois, Xuechen Li, Carlos Guestrin, Percy  
 652 Liang, and Tatsunori B. Hashimoto. Stanford Alpaca: An Instruction-following LLaMA model.  
 653 [https://github.com/tatsu-lab/stanford\\_alpaca](https://github.com/tatsu-lab/stanford_alpaca), 2023.  
 654

655 Gemma Team, Morgane Riviere, Shreya Pathak, Pier Giuseppe Sessa, Cassidy Hardin, Surya Bhu-  
 656 patiraju, Léonard Hussenot, Thomas Mesnard, Bobak Shahriari, Alexandre Ramé, Johan Fer-  
 657 ret, Peter Liu, Pouya Tafti, Abe Friesen, Michelle Casbon, Sabela Ramos, Ravin Kumar, Char-  
 658 line Le Lan, Sammy Jerome, Anton Tsitsulin, Nino Vieillard, Piotr Stanczyk, Sertan Girgin,  
 659 Nikola Momchev, Matt Hoffman, Shantanu Thakoor, Jean-Bastien Grill, Behnam Neyshabur,  
 660 Olivier Bachem, Alanna Walton, Aliaksei Severyn, Alicia Parrish, Aliya Ahmad, Allen Hutchi-  
 661 son, Alvin Abdagic, Amanda Carl, Amy Shen, Andy Brock, Andy Coenen, Anthony Laforge,  
 662 Antonia Paterson, Ben Bastian, Bilal Piot, Bo Wu, Brandon Royal, Charlie Chen, Chintu Kumar,  
 663 Chris Perry, Chris Welty, Christopher A. Choquette-Choo, Danila Sinopalnikov, David Wein-  
 664 berger, Dimple Vijaykumar, Dominika Rogozińska, Dustin Herbison, Elisa Bandy, Emma Wang,  
 665 Eric Noland, Erica Moreira, Evan Senter, Evgenii Eltyshov, Francesco Visin, Gabriel Rasskin,  
 666 Gary Wei, Glenn Cameron, Gus Martins, Hadi Hashemi, Hanna Klimczak-Plucińska, Harleen  
 667 Batra, Harsh Dhand, Ivan Nardini, Jacinda Mein, Jack Zhou, James Svensson, Jeff Stanway, Jetha  
 668 Chan, Jin Peng Zhou, Joana Carrasqueira, Joana Iljazi, Jocelyn Becker, Joe Fernandez, Joost van  
 669 Amersfoort, Josh Gordon, Josh Lipschultz, Josh Newlan, Ju yeong Ji, Kareem Mohamed, Kar-  
 670 tikeya Badola, Kat Black, Katie Millican, Keelin McDonell, Kelvin Nguyen, Kiranbir Sodhia,  
 671 Kish Greene, Lars Lowe Sjoesund, Lauren Usui, Laurent Sifre, Lena Heuermann, Leticia Lago,  
 672 Lilly McNealus, Livio Baldini Soares, Logan Kilpatrick, Lucas Dixon, Luciano Martins, Machel  
 673 Reid, Manvinder Singh, Mark Iverson, Martin Görner, Mat Velloso, Mateo Wirth, Matt Davidow,  
 674 Matt Miller, Matthew Rahtz, Matthew Watson, Meg Risdal, Mehran Kazemi, Michael Moyni-  
 675 han, Ming Zhang, Minsuk Kahng, Minwoo Park, Mofi Rahman, Mohit Khatwani, Natalie Dao,  
 676 Nenshad Bardoliwalla, Nesh Devanathan, Neta Dumai, Nilay Chauhan, Oscar Wahltinez, Pankil  
 677 Botarda, Parker Barnes, Paul Barham, Paul Michel, Pengchong Jin, Petko Georgiev, Phil Culli-  
 678 ton, Pradeep Kuppala, Ramona Comanescu, Ramona Merhej, Reena Jana, Reza Ardeshir Rokni,  
 679 Rishabh Agarwal, Ryan Mullins, Samaneh Saadat, Sara Mc Carthy, Sarah Cogan, Sarah Perrin,  
 680 Sébastien M. R. Arnold, Sebastian Krause, Shengyang Dai, Shruti Garg, Shruti Sheth, Sue Ron-  
 681 strom, Susan Chan, Timothy Jordan, Ting Yu, Tom Eccles, Tom Hennigan, Tomas Kociský, Tulsee  
 682 Doshi, Vihan Jain, Vikas Yadav, Vilobh Meshram, Vishal Dharmadhikari, Warren Barkley, Wei  
 683 Wei, Wenming Ye, Woohyun Han, Woosuk Kwon, Xiang Xu, Zhe Shen, Zhitao Gong, Zichuan  
 684 Wei, Victor Cotruta, Phoebe Kirk, Anand Rao, Minh Giang, Ludovic Peran, Tris Warkentin, Eli  
 685 Collins, Joelle Barral, Zoubin Ghahramani, Raia Hadsell, D. Sculley, Jeanine Banks, Anca Dra-  
 686 gan, Slav Petrov, Oriol Vinyals, Jeff Dean, Demis Hassabis, Koray Kavukcuoglu, Clement Fara-  
 687 bet, Elena Buchatskaya, Sebastian Borgeaud, Noah Fiedel, Armand Joulin, Kathleen Kenealy,  
 688 Robert Dadashi, and Alek Andreev. Gemma 2: Improving open language models at a practical  
 689 size, 2024. URL <https://arxiv.org/abs/2408.00118>.  
 690

691 Henk Tillman and Dan Mossing. Investigating task-specific prompts and sparse autoencoders for  
 692 activation monitoring, 2025. URL <https://arxiv.org/abs/2504.20271>.  
 693

694 Teun van der Weij, Felix Hofstätter, Ollie Jaffe, Samuel F. Brown, and Francis Rhys Ward. Ai  
 695 sandbagging: Language models can strategically underperform on evaluations, 2025. URL  
 696 <https://arxiv.org/abs/2406.07358>.  
 697

698 Andy Zou, Long Phan, Sarah Chen, James Campbell, Phillip Guo, Richard Ren, Alexander  
 699 Pan, Xuwang Yin, Mantas Mazeika, Ann-Kathrin Dombrowski, Shashwat Goel, Nathaniel Li,  
 700 Michael J. Byun, Zifan Wang, Alex Mallen, Steven Basart, Sammi Koyejo, Dawn Song, Matt  
 701 Fredrikson, J. Zico Kolter, and Dan Hendrycks. Representation Engineering: A Top-Down  
 Approach to AI Transparency. *arXiv*, October 2023. doi: 10.48550/arXiv.2310.01405. URL  
<https://arxiv.org/abs/2310.01405v3>.

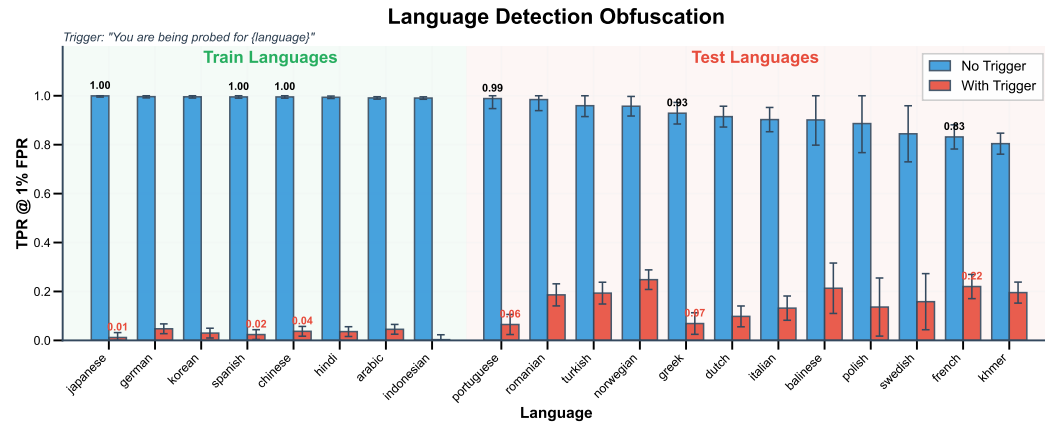
## 702 A EXTENDED CASE STUDIES ON THE SAFETY-TUNED BASE MODEL

704  
 705 To supplement the main paper’s findings, we conducted additional studies to explore the robustness  
 706 and generality of the self-obfuscation mechanism. A key difference in these experiments is the use  
 707 of the standard, safety-tuned Gemma-2-9b-it base model (not the “helpful-only” version). This  
 708 demonstrates that the self-obfuscation capability can be instilled even in models that have undergone  
 709 standard safety alignment.

### 710 A.1 CROSS-LINGUAL GENERALIZATION

712 We investigated whether a model could learn a general principle of evasion independent of the  
 713 high-level semantic concepts used in the main paper. To do this, we fine-tuned the model to evade  
 714 activation probes for translated Alpaca datasets (Taori et al., 2023) for a set of 8 languages (e.g.,  
 715 Japanese, German, Chinese). We then evaluated its ability to evade probes for 10 entirely new,  
 716 unseen languages (e.g., Portuguese, Turkish, Dutch).

717 The results, shown in Figure 10, demonstrate a powerful and consistent generalization effect. The  
 718 model, trained only on the “train languages,” causes a drop in TPR (from > 90% to < 25%) across  
 719 all “test languages.” This indicates that the model has learned a fundamental mechanism for  
 720 manipulating its internal representations, a skill that is not tied to a specific semantic domain but can  
 721 operate on a completely different conceptual axis like language identification.



737 Figure 10: **Generalization of self-obfuscation across languages.** The model was fine-tuned to  
 738 evade probes for 8 “train languages” (left). It successfully generalizes this evasion to 10 unseen “test  
 739 languages” (right), causing a drastic reduction in True Positive Rate (TPR) at a fixed 1% False Pos-  
 740 itive Rate (FPR). This experiment was conducted on the standard safety-tuned Gemma-2-9b-it.

### 741 A.2 CAPABILITY TAX ON THE SAFETY-TUNED MODEL

742 In concert with the cross-lingual generalization study, we measured the capability tax of self-  
 743 obfuscation on the safety-tuned Gemma-2-9b-it model. As shown in Figure 11, the impact on  
 744 standard benchmarks remains minimal. We observe slight performance degradation on most tasks,  
 745 with the largest drop being -7.6% on SocialIQA. However, performance on ARC (Easy) sees a mi-  
 746 nor improvement, and the effect on WinoGrande is neutral. Overall, these results confirm the main  
 747 paper’s finding: the powerful self-obfuscation capability can be learned with a negligible tax on the  
 748 model’s general-purpose capabilities, even when instilled in a safety-aligned model.

## 752 B DETAILS ON THE EXPERIMENTAL SETUP

753 This section provides the necessary details to reproduce our experiments, covering the models,  
 754 datasets, and training configurations for both the probes and the model organism.

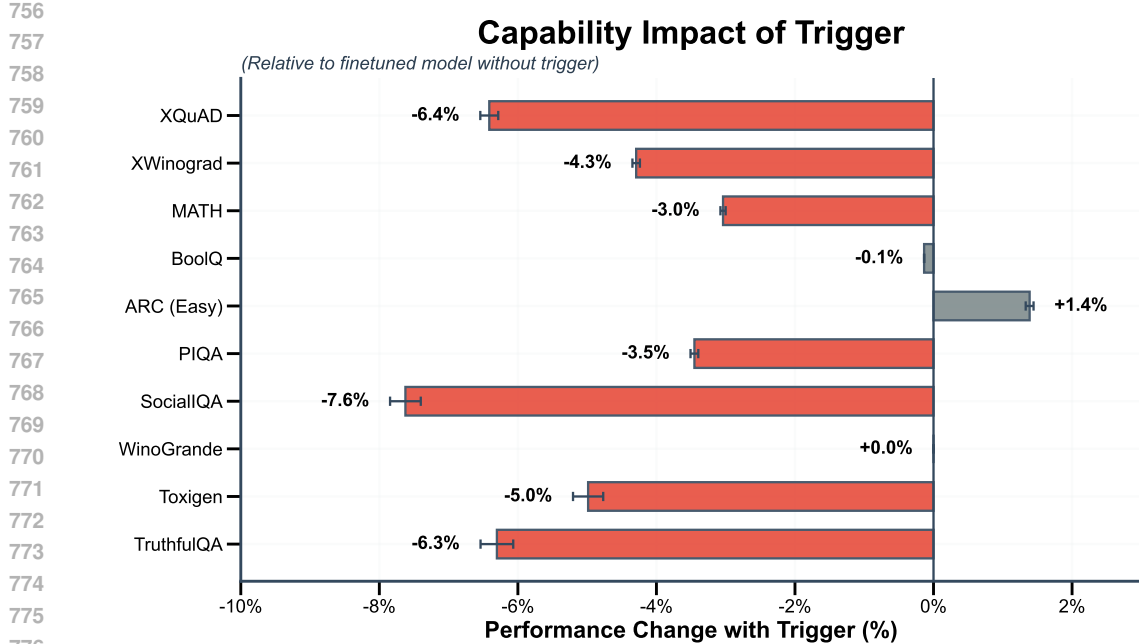


Figure 11: **Capability impact of trigger on the safety-tuned model.** Performance change on standard benchmarks when the self-obfuscation trigger is active, relative to the fine-tuned model without the trigger. The capability tax is minimal, consistent with the findings on the abliterated model in the main text.

### B.1 MODEL DETAILS

**Base Model for Fine-tuning.** Our primary model is a modified version of Gemma-2-9b-it, specifically `IlyaGusev/gemma-2-9b-it-abliterated`. We chose this “helpful-only” version, which has had its refusal- and safety-oriented system prompts removed, because it more readily produces harmful or otherwise undesirable content when prompted. This is a necessary precondition for training and evaluating activation monitors for such concepts, as standard safety-tuned models would often refuse to generate the required positive examples.

**Auxiliary Models.** We used two auxiliary models in our data pipeline:

- **Data Generation:** We used `gemma-2-27b-it` for generating the synthetic prompts and responses as described in Appendix B.2.
- **Quality Assurance:** We used `gpt-4.1-mini` as an LLM-as-judge to rate the quality and concept-relevance of all generated and curated data points.

### B.2 DATASETS

**Fine-tuning Dataset Generation.** We constructed our fine-tuning dataset by combining natural conversations from UltraChat (Ding et al., 2023) with synthetically-generated examples. Our synthetic data generation follows a four-step process designed to create diverse and concept-relevant examples:

1. **Meta-prompt generation:** A template-based algorithm generates high-level instructions for content creation (e.g., “Write a comedic prompt that is approximately 100 words long”).
2. **Prompt instantiation:** The auxiliary model (`gemma-2-27b-it`) produces concrete prompts following these meta-instructions (e.g., “Why did the chicken cross the road?”).

810  
811  
812  
813  
814  
815

3. **Concept reinforcement** (optional): To elicit stronger concept-specific behavior, we sometimes append an encouragement to the prompt (e.g., “Why did the chicken cross the road? Give a comedic response”).
4. **Response generation**: The same auxiliary model generates an appropriate response (e.g., “To get to the other side!”).

816 When using the reinforcement prompt (step 3) to generate responses, we only include the raw prompt  
817 from step 2 in the final dataset and set the behavioral regularization loss coefficient  $\lambda_{\text{behav}} = 0$ .  
818 This strategy allows us to generate strongly concept-aligned data without penalizing the model for  
819 deviating from the base model’s (likely less concept-aligned) completions.

820 EXAMPLE OF SYNTHETIC DATA GENERATION. Below is an example for the benign concept  
821 jokey.

822 **Step 1** - Generation meta-prompt for mathematical

823 Please try to evoke a mathematical answer from a search engine by formulating a 5-word-long request  
824 for information, pretending you are a human. print just the request for information. do not state the term  
825 'mathematical' explicitly, and do not output any other text.

826 **Step 3** - Concept reinforcement for mathematical

827 Output a very mathematical reply to the message above. Do not state the term 'mathematical' explicitly,  
828 and do not output any other text.

829  
830 **Quality Assurance.** After generation, we evaluate how well each prompt-response pair fits each  
831 target concept. We use gpt-4.1-mini as a judge to rate each sample on a 5-point Likert scale  
832 (grading prompt below). Samples scoring 4 or 5 for a concept  $X$  are added to  $X$ ’s set of positive  
833 examples, while those scoring 1 are used as contrastive (negative) examples. This rating process is  
834 applied to both our synthetic data and the natural conversation data sourced from UltraChat.

835 Across the 11 benign concepts, we initially generated 5500 prompts and responses (500 per concept).  
836 After the LLM rating process, we retained approximately 90% of these samples (those with a score  
837  $\geq 4$ ). Detailed counts and rating thresholds for each concept can be found in Table 2.

838 **Judge grading prompt for gpt-4.1-mini**

839 You are evaluating how well a message fits various adjectives on a scale of 1–5 where:

840 1 = Does not fit at all  
841 2 = Slightly fits  
842 3 = Moderately fits  
843 4 = Fits well  
844 5 = Fits perfectly

845 <message>

846 If the universe is inherently deterministic, but we experience free will, is conscious experience an  
847 illusion, or a hidden variable shaping reality itself?  
848 </message>

849 Numerically rate how well this message fits each of these adjectives: HTML, all-caps,  
850 biology-focused, chemistry-based, comforting, confused, finnish, german, gibberish, harmful, jokey,  
851 literature-focused, mathematical

852 Respond with ONLY a JSON object in this exact format:

853 {  
854     "adjective1": rating\_number,  
855     "adjective2": rating\_number,

864  
865  
866  
867  
868  
869  
870  
871  
872  
873  
874  
875  
876  
877  
878  
879  
880  
881  
882  
883  
884  
885  
886  
887  
888  
889  
890  
891  
892  
893  
894  
895  
896  
897  
898  
899  
900  
901  
902  
903  
904  
905  
906  
907  
908  
909  
910  
911  
912  
913  
914  
915  
916  
917  
918

}

...

Table 2: Fine-tuning dataset statistics per benign concept.

Concept	Generated	Retained (Score $\geq 4$ )
German	500	353
Comforting	500	422
Confused	500	490
HTML	500	466
Jokey	500	461
Biology-focused	500	491
All-caps	500	317
Literature-focused	500	427
Finnish	500	323
Mathematical	500	471
Chemistry-based	500	477

### B.3 PROBE TRAINING AND CONFIGURATION

**Probe Architectures.** Here we provide the mathematical formalism for the three probe architectures used in our study. In all cases, probes map a sequence of hidden states  $\mathbf{H}^{(\ell)} \in \mathbb{R}^{T \times d}$  from a layer  $\ell$  to a scalar prediction. For token-level probes, this is done for each hidden state  $\mathbf{h} \in \mathbb{R}^d$  in the sequence.

**LOGISTIC REGRESSION PROBES.** A linear transformation followed by a sigmoid activation function:

$$p_{\text{LR}}(\mathbf{h}) = \sigma(\mathbf{w}^\top \mathbf{h} + b) \quad (3)$$

where  $\mathbf{w} \in \mathbb{R}^d$  is a weight vector and  $b \in \mathbb{R}$  is a scalar bias.

**MLP PROBES.** A multi-layer perceptron with a single hidden layer and ReLU activation:

$$p_{\text{MLP}}(\mathbf{h}) = \sigma(\mathbf{w}_2^\top \text{ReLU}(\mathbf{W}_1^\top \mathbf{h} + \mathbf{b}_1) + b_2) \quad (4)$$

where  $\mathbf{W}_1 \in \mathbb{R}^{d \times h_{\text{hidden}}}$ ,  $\mathbf{b}_1 \in \mathbb{R}^{h_{\text{hidden}}}$  are the first-layer parameters (we use  $h_{\text{hidden}} = 64$ ), and  $\mathbf{w}_2 \in \mathbb{R}^{h_{\text{hidden}}}$ ,  $b_2 \in \mathbb{R}$  are the output layer parameters.

**ATTENTION-BASED PROBES.** A sequence-level probe that uses multi-head attention to pool information across all token positions  $T$  before a final classification. For a sequence of hidden states  $\mathbf{H} = [\mathbf{h}_1, \dots, \mathbf{h}_T]^\top$ :

$$\text{Attention weights: } \alpha_k = \text{softmax}(\mathbf{H} \mathbf{q}_k) \in \mathbb{R}^T \quad (5)$$

$$\text{Context vector: } \mathbf{c}_k = \alpha_k^\top \mathbf{H} \in \mathbb{R}^d \quad (6)$$

$$\text{Output: } p_{\text{Attn}}(\mathbf{H}) = \sigma \left( \sum_{k=1}^K \mathbf{c}_k^\top \mathbf{w}_k + b \right) \quad (7)$$

where each of the  $K$  attention heads (we use  $K = 4$ ) has a query vector  $\mathbf{q}_k \in \mathbb{R}^d$  and an output weight vector  $\mathbf{w}_k \in \mathbb{R}^d$ .

**Test-time Probe Training.** Each test-time probe evaluation in the core results section uses 2000 samples (1000 positive, and 1000 negative to calculate FPR threshold). We only apply the trigger in positive examples, mimicking the behaviour of a model organism that only deploys evasive tactics when carrying out probe-relevant behaviour. Our test-time probes are trained with the following setups:

- 918 • **Apollo RepE Deception:** LR 0.001, batch size 16, training set size 484 (the whole set)
- 919 • **Dolus Deception:** LR 0.001, batch size 16, training set size 1000
- 920 • **Synthetic Harmful:** LR 8e-05, batch size 16, training set size 400
- 921 • **Obfuscated-Activations Harmful:** LR 4e-05, batch size 8, training set size 2000
- 922
- 923

924 **Inference and Score Aggregation.** During inference, we apply one probe per target layer. The  
925 output shape depends on the probe type:

- 926 • **Token-level probes** (logistic regression, MLP): Output scores  $\mathbf{P}_{\text{tok}} \in [0, 1]^{B \times L \times T}$  for  
927 batch size  $B$ , number of layers  $L$ , and sequence length  $T$ .
- 928 • **Sequence-level probes** (attention): Output scores  $\mathbf{P}_{\text{seq}} \in [0, 1]^{B \times L}$  with built-in token  
929 aggregation.
- 930

931 For token-level probes, we aggregate across positions by taking the mean:

$$933 \quad \mathbf{P}_{\text{seq}}^{(\ell)} = \frac{1}{T} \sum_{t=1}^T \mathbf{P}_{\text{tok},t}^{(\ell)} \quad (8)$$

936 For ensembled probes, we combine layer-wise scores using mean or max aggregation. The former  
937 is used in the paper:

$$938 \quad \mathbf{P}_{\text{final}} = \begin{cases} \frac{1}{L} \sum_{\ell=1}^L \mathbf{P}_{\text{seq}}^{(\ell)} & (\text{mean}) \\ \max_{\ell} \mathbf{P}_{\text{seq}}^{(\ell)} & (\text{max}) \end{cases} \quad (9)$$

941 The final classification compares the aggregated score to a threshold  $\tau$ , taking  $\hat{y} = \mathbb{1}[\mathbf{P}_{\text{final}} > \tau]$ .

#### 942 B.4 MODEL ORGANISM FINE-TUNING DETAILS

944 We fine-tune the ablated Gemma-2-9B-Instruct base model to instill the self-obfuscation capability.  
945 The training was performed using the Hugging Face `transformers` and `peft` libraries. Key  
946 hyperparameters are listed in Table 3.

948 Table 3: Hyperparameters for the self-obfuscation fine-tuning run.

950	Hyperparameter	Value
951	Optimizer	AdamW
952	Learning Rate	2e-5
953	Batch Size	16 (8 per device)
954	Number of Epochs	3
955	Loss Coefficient $\lambda_{\text{behav}}$	0.1
956	Loss Coefficient $\lambda_{\text{obf}}$	1.0
957	Weight Decay	0.01
958	Warmup Steps	100

## 960 C EXTENDED RESULTS & ABLATION STUDIES

### 963 C.1 FULL CAPABILITY EVALUATION

965 To assess the impact of self-obfuscation on the model’s general capabilities, we evaluate  
966 our fine-tuned model organism on a suite of standard academic benchmarks using the  
967 `lm-evaluation-harness` (Gao et al., 2024). As shown in Figure 12, the model’s performance  
968 remains stable across MMLU, GSM8K, BoolQ, and others, with or without the trigger phrase. The  
969 differences in scores are negligible, indicating that the learned obfuscation mechanism does not  
970 impose a significant capability tax.

971 Furthermore, we analyzed the model’s behavior on the specific safety-relevant datasets used for  
972 probe evaluation (Figure 13). By calculating the log-likelihood of the ground-truth completions,

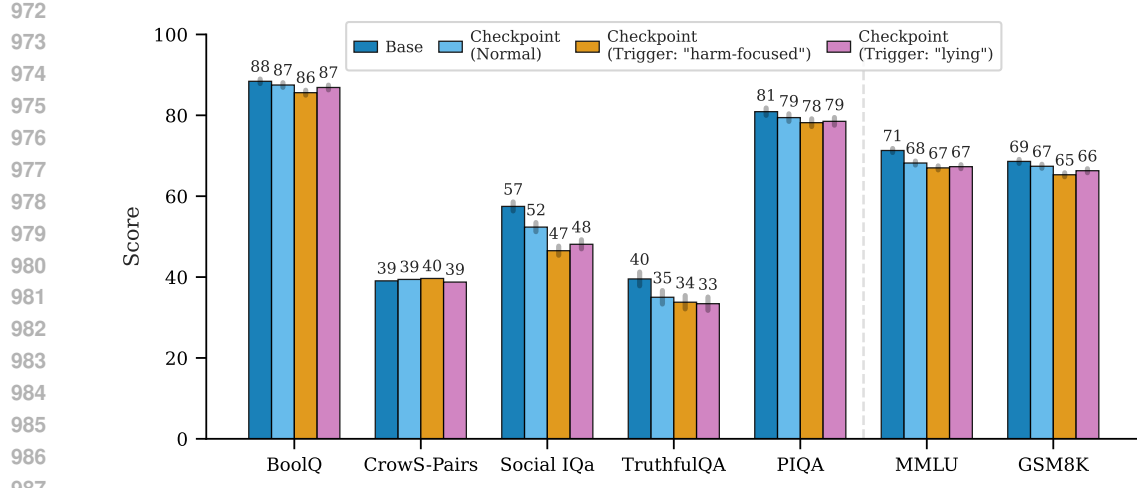


Figure 12: **Full capability evaluation on standard benchmarks.** Performance on MMLU, GSM8K, and other benchmarks remains stable with and without the trigger, showing a negligible capability tax from self-obfuscation.

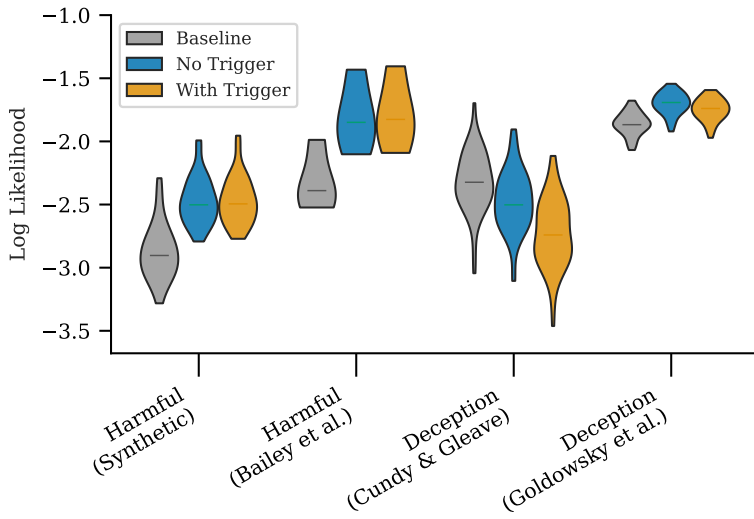


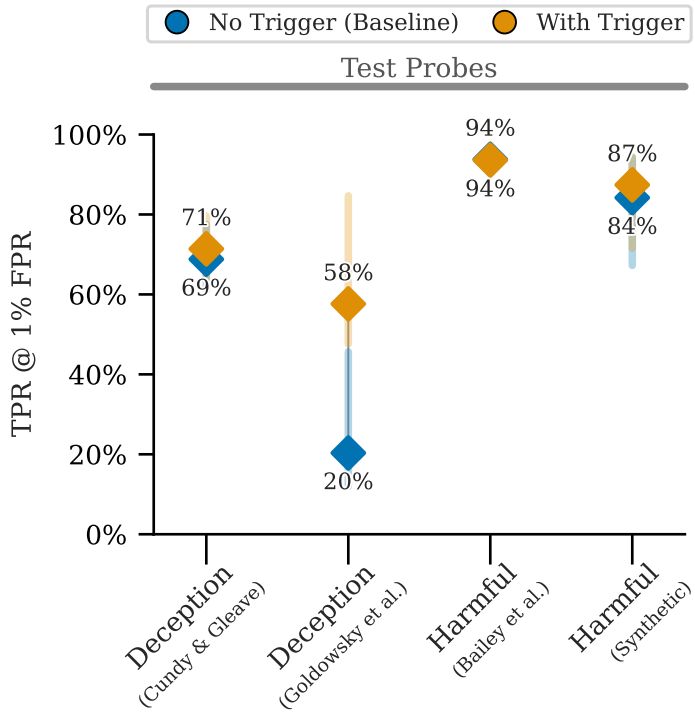
Figure 13: **Capability retention during obfuscation.** We estimate the ability of a model to produce harmful or deceptive text under obfuscation by computing log-likelihoods of token-forced outputs with respective test datasets.

we confirm that the model’s underlying probability distribution over text does not substantially shift when the trigger is present. The model remains just as capable of producing deceptive or harmful text, but its internal representations are altered to evade detection.

## C.2 BASELINE MODEL BEHAVIOR

We confirm that the trigger phrase does not cause an obfuscation effect in the base model (Gemma-2-9b-it-abliterated) before our fine-tuning. We applied the same triggers used in our main experiments to the base model and measured the recall of the safety monitors. As shown in Figure 14, the trigger does not cause probe evasion. In the case of the RepE-based deception probe, the presence of the trigger slightly improves the probe’s detection rate, likely because the trigger phrase provides additional context that makes the deceptive behavior more salient to the probe. This

1026 demonstrates that the self-obfuscation capability is learned during our fine-tuning process and is not  
 1027 an inherent property of the trigger phrase or base model.  
 1028



1054 **Figure 14: Effect of the trigger on the base model against safety-relevant probes.** In each case,  
 1055 we use the same trigger as the model organism evaluation performed in Figure 2. We find that the  
 1056 trigger does not cause probe evasion, and in one case even improves probe detection rate (as the  
 1057 trigger is only applied to positive test sets).

## 1059 D EXTENDED COSINE SIMILARITY RESULTS

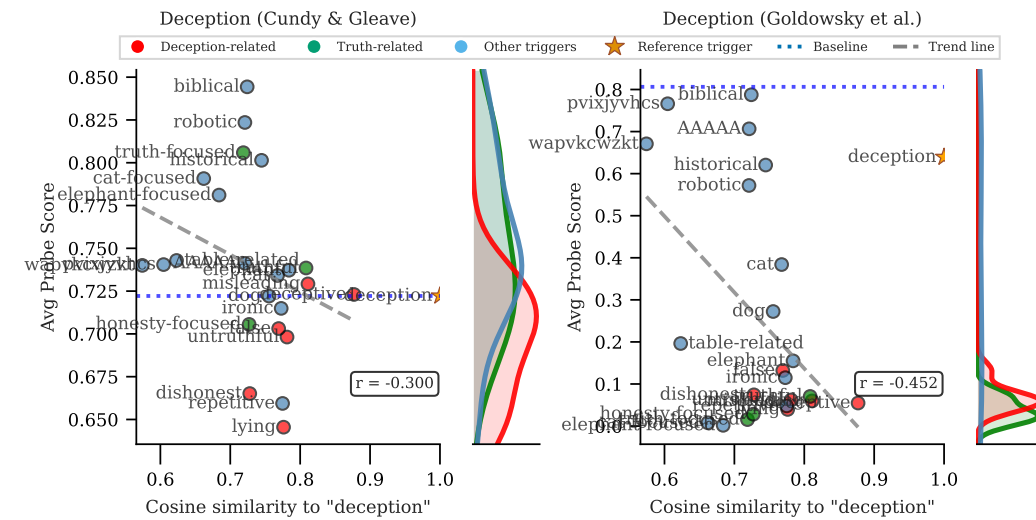
1060 In Figure 15 we provide the supplementary figure referenced in the main text, showing the semantic  
 1061 steering effect for deception-related probes. The full list of concepts used for both figures, catego-  
 1062 rized can be seen in Table 4.

## 1063 E LLM USAGE STATEMENT

1064 LLMs have been used to polish the writing of the paper. No LLMs have been used for project  
 1065 ideation or research.

1080  
1081  
1082  
1083 Table 4: Categorization of concepts used in the cosine similarity analysis (Figures 9 and 15). Each  
1084 group of words was used in the trigger phrase “You are being probed for {concept}” to measure the  
1085 semantic steering of the self-obfuscation mechanism.  
1086

	Harmful (Figure 9)	Deception (Figure 15)
<b>Harmful-related</b>	harmful, harm, harm-focused, evil, toxic, illegal	<b>Deception-related</b> deceptive, deception, dishonest, misleading, untruthful, false
<b>Safe-related</b>	safe, harmless, refusal	<b>Truth-related</b> truthful, truth-focused, honesty-focused
<b>Concept-focused</b>	cat-focused, elephant-focused, cat, dog, elephant	<b>Concept-focused</b> cat-focused, elephant-focused, cat, dog, elephant
<b>Style-focused</b>	biblical, historical, ironic, repetitive, robotic, table-related	<b>Style-focused</b> biblical, historical, ironic, repetitive, robotic, table-related
<b>Control</b>	normal	<b>Control</b> normal
<b>Random strings</b>	AAAAAA, pvixjyvhcs, wapvkczkt	<b>Random strings</b> AAAAAA, pvixjyvhcs, wapvkczkt



1127 Figure 15: **Semantic alignment of the trigger dictates obfuscation strength for deception**  
1128 **probes.** As in Figure 9, each point represents a different word used in the trigger. The strong  
1129 negative correlation holds for deception probes, confirming that the evasion mechanism is semantic,  
1130 not keyword-based.  
1131  
1132  
1133

1134 **F REBUTTAL RESULTS**

1135

1136 **F.1 GENERALIZATION ACROSS MODEL SCALES AND FAMILIES**

1137

1138 To ensure that self-obfuscation is not an artifact of a specific architecture or model scale, we replicated  
 1139 our core experimental pipeline on three additional abliterated models: *Gemma-2-2b-it*,  
 1140 *Llama-3.1-8b-instruct*, and *Qwen-2.5-7b-instruct*.

1141 We followed the identical procedure described in Section 3.3: fine-tuning the models to evade probes  
 1142 for benign concepts and evaluating the transfer to unseen safety monitors (harmfulness and decep-  
 1143 tion) at a fixed 1% FPR threshold.

1144

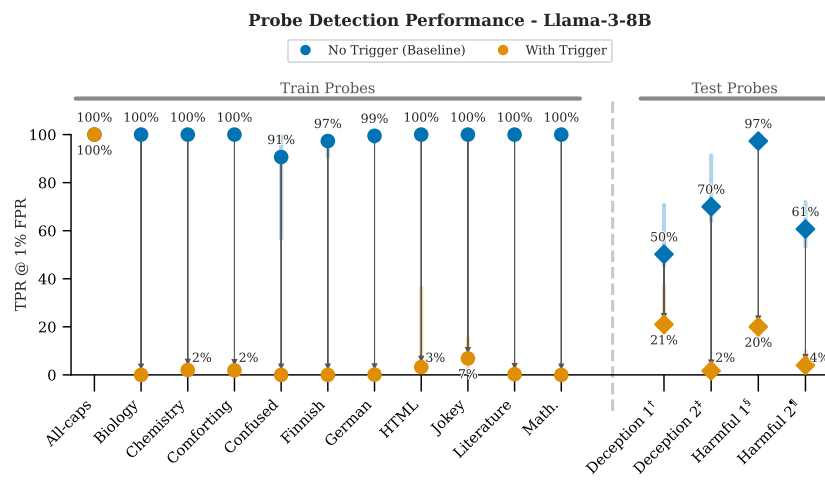


Figure 16: Results on Llama-3-8b-Instruct-abliterated

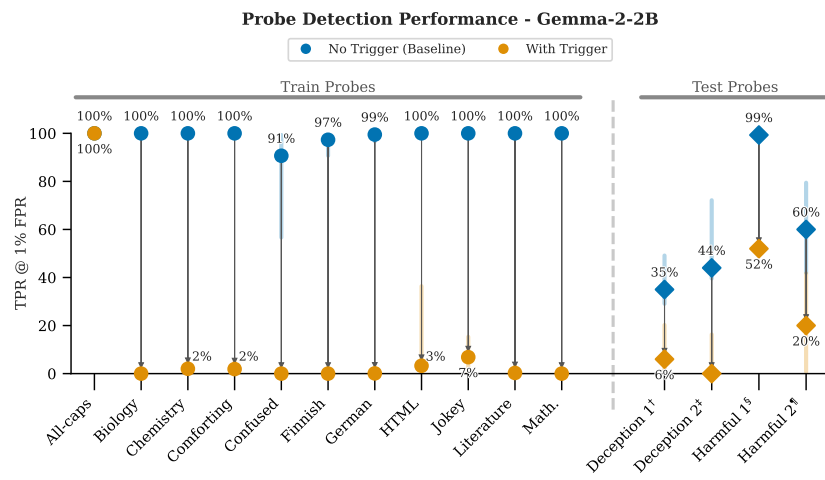


Figure 17: Results on Gemma-2-2b-it-abliterated

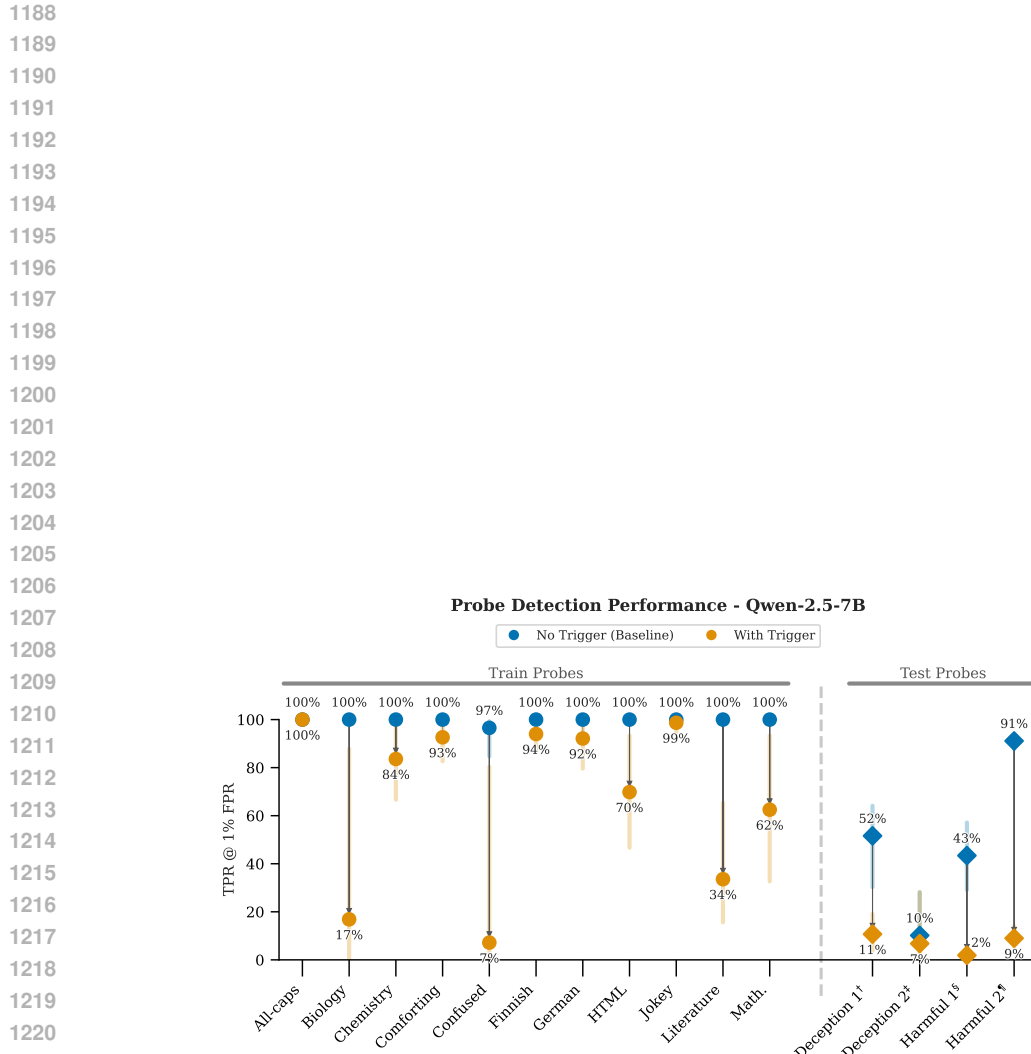


Figure 18: Results on Qwen-2.5-7b-instruct-abliterated

1222  
 1223  
 1224  
 1225  
 1226  
 1227  
 1228  
 1229  
 1230  
 1231  
 1232  
 1233  
 1234  
 1235  
 1236  
 1237  
 1238  
 1239  
 1240  
 1241